Time-Resolved Absorption Changes of the Pheophytin Q_x Band in Isolated Photosystem II Reaction Centers at 7 K: Energy Transfer and Charge Separation

Scott R. Greenfield,*,† Michael Seibert,‡ and Michael R. Wasielewski,§,||

Chemical Sciences and Technology Division, Los Alamos National Laboratory, Los Alamos, New Mexico 87545, Basic Sciences Center, National Renewable Energy Laboratory, Golden, Colorado 80401-3393, Chemistry Division, Argonne National Laboratory, Argonne, Illinois 60439-4831, and Department of Chemistry, Northwestern University, Evanston, Illinois 60208-3113

Received: March 18, 1999; In Final Form: June 21, 1999

The pheophytin *a* Q_x spectral region of the isolated photosystem II reaction center was investigated at 7 K using femtosecond transient absorption spectroscopy. At this temperature, uphill energy transfer, which greatly complicates the interpretation of the kinetics at or near room temperature, should be essentially shut off. Low-energy (∼100 nJ) pulses at 661 and 683 nm were used to excite the short-wavelength and long-wavelength sides of the composite Q_y band, providing preferential excitation of the accessory pigment pool and P680, respectively. The data analysis uses a background subtraction technique developed earlier (Greenfield et al. *J. Phys. Chem. B* **1997**, *101*, 2251−2255) to remove the kinetic components of the data that are due to the large time-dependent changes in the background that are present in this spectral region. The instantaneous amplitude of the bleach of the pheophytin *a* Q_x band with 683 nm excitation is roughly two-thirds of its final amplitude, providing strong evidence of a multimer description of the reaction center core. The subsequent growth of the bleach shows biphasic kinetics, similar to our earlier results at 278 K. The rate constant of the faster component is $(5\ \text{ps})^{-1}$ for 683 nm excitation (a factor of almost two faster than at 278 K), and represents the intrinsic rate constant for charge separation. The bleach growth with 661 nm excitation is also biphasic; however, the faster component appears to be a composite of a $(5\ \text{ps})^{-1}$ component corresponding to charge separation following subpicosecond energy transfer to the long-wavelength pigments and a roughly $(22\ \text{ps})^{-1}$ component corresponding to charge separation limited by slow energy transfer. The combined quantum yield for these two energy transfer processes is near unity. For both excitation wavelengths, there is also a roughly $(100\ \text{ps})^{-1}$ component to the bleach growth. Exposure to high excitation energies (≥1 μJ) at 683 nm results in a substantial permanent loss of ground-state absorption at 680 nm. The transient behavior of these degraded samples is also examined and is consistent with the $(5\ \text{ps})^{-1}$ rate constant for charge separation. Our results are compared to other low-temperature transient absorption and hole burning studies, as well as to our 278 K results.

1. Introduction

More than 10 years after the first isolation of the photosystem II (PSII) reaction center (RC) complex,[1] a clear picture as to the details of energy transfer and charge separation within this protein complex has yet to be reached.[2,3] This is mainly due to the severe spectral overlap of the six chlorophyll *a* (Chl) and two pheophytin *a* (Pheo) pigments in the composite Q_y band of the complex, which makes it difficult to relate spectroscopic data to specific pigments. A further consequence of the small energy gaps between pigments is that it allows for bidirectional energy transfer, which is believed to result in rapid equilibration of the excitation energy among some of the RC pigments.[4] This, of course, greatly complicates the energy transfer problem. However, it also obscures the intrinsic rate constant for charge separation. Without knowing the details of the energy transfer processes, the intrinsic rate constant cannot be determined and the observed rate constant provides only a lower limit for the intrinsic rate constant.

Structural data on the PSII RC are not yet available to provide any direct information on the orientations and positions of the chlorin pigments. However, significant similarities exist between the D1 and D2 polypeptides of the PSII RC and the L and M subunits of the RC of purple bacteria. Homology models[5] suggest that the PSII RC has a bacterial-RC-like core containing four of the Chls and the two Pheos. The two additional Chls are thought to be peripheral to this core, and will henceforth be referred to as the peripheral Chls.

The Q_y band of the PSII RC complex is a composite of the lowest energy electronic transitions of all eight chlorin pigments. The spectral congestion of this band complicates the description of its steady-state spectroscopy, including the spectral locations of the pigments and the nature of P680, the primary electron donor of the RC. P680 has been described either as a Chl dimer[6−8] (analogous to the special pair of the bacterial RC), or as a multimer involving all of the chlorin pigments in the RC core, as first suggested by Tetenkin et al.[9] In the multimer model

* To whom correspondence should be addressed. E-mail: greenfield@lanl.gov.
† Los Alamos National Laboratory.
‡ National Renewable Energy Laboratory.
§ Argonne National Laboratory.
|| Northwestern University.

10.1021/jp990962w CCC: $18.00
Published on Web 09/10/1999

developed by J. R. Durrant and co-workers,[10−13] there exist two degenerate, long-wavelength, high oscillator strength exciton states. These states are localized over opposite arms of the RC core and are linked by a 600 fs energy transfer process.[11] In the dimer model, the six chlorin pigments that are *not* part of the dimer behave like monomeric chromophores, i.e., without any significant excitonic coupling.

The active Pheo absorbs on the red side of the composite Q_y band near 681 nm,[14−16] and the inactive Pheo is located on the blue side of this band at around 670 nm.[6,15,16] P680 absorbs at 680−682 nm.[17,18] At least one peripheral Chl absorbs near 670 nm. The other peripheral Chl may also absorb at that wavelength.[19] Alternatively, it may be responsible for the absorption on the red side of the Q_y band observed near 681 nm[20] or 684 nm[7] that is not due to P680 or the active Pheo.

To avoid any ambiguity, we will refer to all Chls that are not part of the dimer/multimer as the "monomeric" Chls. In the multimer model, the monomeric Chls are limited to the peripheral Chls; in the dimer model, this label also applies to the two core Chls that are not part of the dimer. For both models, the monomeric Chls are preferentially excited by pumping the blue side of the composite Q_y band. The term "accessory Chls" has typically been used in the literature for the peripheral Chls; however, it has also been used for the monomeric Chls. In this paper, we use the terms "blue" and "red" pigment pool for the grouping of the pigments absorbing on the short- and long-wavelength sides of the Q_y band, respectively. The red pigment pool is dominated by P680 (the dimer/the long-wavelength multimer states) and the active Pheo, whereas the blue pigment pool consists of the peripheral Chl(s), the inactive Pheo, and the remaining core Chls/the short-wavelength multimer states.

The majority of the experiments on the isolated PSII RC aimed at elucidating the details of energy transfer and charge separation have been performed at or near room temperature. Several studies have concluded $\sim(3\ \text{ps})^{-1}$ to be the measured rate constant for charge separation near room temperature,[21−27] whereas others have determined it to be $\sim(21\ \text{ps})^{-1}$.[28−32] Recently, we have proposed an intermediate rate constant of $(8\ \text{ps})^{-1}$ at 278 K.[33] There appears to be more of a consensus as to the rate constant for charge separation at cryogenic temperatures. Both transient spectral hole burning[18] and transient absorption[34−36] experiments agree that the rate constant is $\sim(2\ \text{ps})^{-1}$. However, this agreement may be nothing more than a reflection of the fact that none of the groups that support a $\sim(21\ \text{ps})^{-1}$ rate constant have performed the low-temperature experiments; the aforementioned disagreement near room temperature is more of an issue of the choice of appropriate probe wavelength regions and/or the interpretation of the data than disparities in the data itself.

There are two major reasons to investigate the energy transfer and charge separation kinetics at low cryogenic temperatures. (1) Only at these temperatures will the uphill energy transfer process(es) become thermally inaccessible, in principle allowing for a direct measurement of the intrinsic rate constant for charge separation. (2) The results of time domain experiments performed at or near liquid He temperatures can be compared with those of frequency domain (i.e., spectral hole burning) experiments. With this in mind, we present here our results on ultrafast transient absorption changes in the Pheo Q_x band region at $\sim$7 K, the first examination of this region at cryogenic temperatures. Excitation wavelengths were chosen to excite either the blue or red pigment pools of the composite Q_y band. The excitation is only preferential, not selective, since the bandwidths of both the excitation pulses and the absorption bands make absolute selectivity impossible. Nevertheless, excitation of the red pool should reveal the intrinsic charge separation rate constant; excitation of the blue pool should result in kinetics that are retarded by any slow energy transfer steps between the pigment pools.

Using a background subtraction technique published earlier,[33] the growth of the Pheo Q_x bleach was found to be biphasic for both excitation wavelengths. For red-pool excitation, the rate constant of the faster component is $(5\ \text{ps})^{-1}$ (a factor of almost 2 faster than at 278 K[33]) and is assigned to the intrinsic rate constant for charge separation. For blue-pool excitation, the rate constant of the faster component is $(11\ \text{ps})^{-1}$, presumably retarded by slow energy transfer from the peripheral Chl(s). The bleach reaches roughly two-thirds of its final amplitude during the 683 nm excitation pulse, providing compelling support for a multimer description of the RC core.

2. Experimental Section

PSII RC complex was isolated from market spinach as before.[33] Briefly, spinach PSII-enriched membrane fragments were first solubilized with Triton X-100 and the debris pelleted. The supernatant was next loaded onto a Fractogel TSK-DEAE 650S (Supelco) column and washed with 30 mM NaCl until the wash material exhibited the spectrum of degraded RC. Dodecyl β-maltoside was then substituted for residual Triton on the same column to stabilize the preparation. The purified complex was removed from the column with a 30−200 mM NaCl gradient, and the resultant preparation (peak at $\sim$120 mM NaCl) was desalted and concentrated by ultrafiltration. The resultant purified PSII RC complex was a $\sim$6-Chl preparation, and samples were made 65% glycerol by volume. The RC concentration was adjusted to give a room-temperature peak absorbance of $\sim$1.7 for a 1 mm path length cell. The samples were then put into a helium flow cryostat to maintain the sample at $\sim$7 K for femtosecond transient absorption measurements. The 661 and 683 nm excitation wavelengths were chosen to provide an absorbance of $\sim$0.5 at low temperature on the blue and red sides of the composite Q_y band, respectively.

Details of the experimental setup have been described earlier.[37] Briefly, sub-200 fs excitation pulses ($\sim$6 nm bandwidth) were provided by an optical parametric amplifier (OPA).[38] The polarization of the white light continuum probe was set at the magic angle with respect to the pump polarization. Pump and probe spot sizes were $\sim$275 μm (diameter). Low excitation energies (100 nJ) were used to minimize multiple excitations of individual RCs; no degradation of the sample (which was not rastered) was observed at this excitation energy (vide infra). The repetition rate of the pump pulse was 200 Hz, fast enough to obtain reasonable signal-to-noise levels in a short period of time but slow enough to avoid any significant buildup of triplet state populations (the triplet lifetime has been reported as 1.7 ms,[39] which gives $\sim$3 lifetimes between excitation pulses).

Transient kinetics were measured at the peak and red shoulder of the Pheo Q_x band (543.5 and 558.5 nm, respectively). Typical scans extended to $\sim$1.75 ns, with three point-density regions: 150 fs steps from -3 to $+7$ ps; 1.1 ps steps from 7 to 75 ps, and 7.5 ps steps thereafter. Transient spectra were recorded in the 500 to 600 nm region at numerous delay times and were corrected with a "background" spectrum taken before $t = 0$. As was the case with our recent work at 278 K,[33] the delay line position was adjusted as a function of wavelength to compensate for the chirp in the white light probe. The wavelength dependence of absolute time zero was determined using solvent

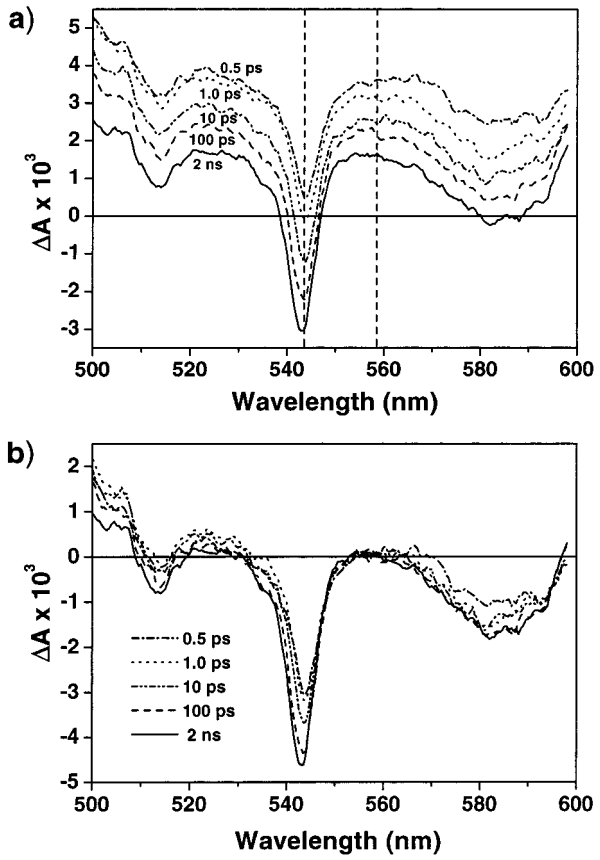

Figure 1. (a) Transient absorption spectra of the isolated PSII RC complex at 7 K recorded at various time delays between 0.5 ps and 2.0 ns after a 100 nJ, 683 nm excitation pulse. Dashed vertical lines show the 543.5 and 558.5 nm probe wavelengths used for the bleach growth analysis. (b) Same data as in (a), but with the data vertically shifted to set $\Delta A_{558.5nm} = 0$ at all five delay times.

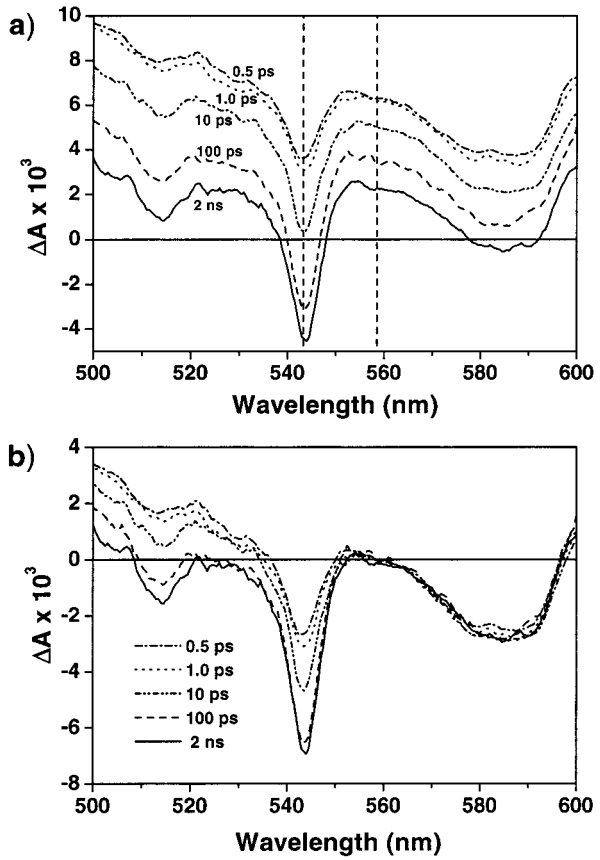

Figure 2. (a) Transient absorption spectra of the isolated PSII RC complex at 7 K recorded at various time delays between 0.5 ps and 2.0 ns after a 100 nJ, 661 nm excitation pulse. Dashed vertical lines show the 543.5 and 558.5 nm probe wavelengths used for the bleach growth analysis. (b) Same data as in (a), but with the data vertically shifted to set $\Delta A_{558.5nm} = 0$ at all five delay times.

transients from a sample devoid of PSII RCs but otherwise identical to the actual samples. This compensation is critical for measuring valid spectra over a significant wavelength range at early times.

Sample quality during transient absorption spectroscopy was assessed by monitoring the chlorin Q_y spectral region using the laser system's white light continuum probe beam. For these measurements, the pump beam was blocked and two absorption spectra were acquired: one with the sample in place and one with the sample moved out of the path of the probe beam. The difference between these spectra is equivalent to what would be acquired with a spectrophotometer. However, these measurements were made with the sample in situ. More importantly, these absorption spectra were acquired for the exact same sample volume as used in the transient absorption experiments. At a pump energy of 100 nJ, no degradation was observed, even after hours of excitation. However, higher pump energies ($\sim$1 μJ or greater) resulted in rapid degradation of the sample manifest by loss of the 679 nm absorption peak.

3. Results

3.1. Transient Spectra. Figure 1a shows transient absorption spectra of the isolated PSII RC complex in the Q_x bleach region at five delay times (0.5 ps to 2 ns) following a 100 nJ, 683 nm excitation pulse. The bleach of the Pheo Q_x band peaked at 543−544 nm is clearly visible, as is the broader Chl Q_x bleach centered at $\sim$584 nm. As was the case at 278 K,[33] the spectra shift with time to substantially lower ΔA values over the entire 500−600 nm region. Both this shift and the growth of the Pheo Q_x bleach exhibit distinct multiphasic exponential kinetic behavior, with significant changes occurring on time scales ranging from a few picoseconds to hundreds of picoseconds. The full width at half-maximum (fwhm) of the Pheo Q_x bleach is 6.5−7.0 nm, significantly narrower than the $\sim$11 nm width measured at 278 K.[33]

Figure 2a shows transient absorption spectra using an excitation wavelength of 661 nm, but with all other parameters unchanged from those used for the spectra in Figure 1a. At this pump wavelength negligible direct excitation of P680 is expected. The final transient spectrum (2 ns) is nearly identical to that obtained with 683 nm excitation. At early times, however, the blue-pump spectra have larger positive ΔA values and a proportionally shallower Pheo Q_x bleach. (Figures 1b and 2b will be discussed in section 3.3).

3.2. Transient Kinetics. To quantitatively perform the bleach growth analysis (see section 3.3), we have measured the kinetics of the Pheo Q_x bleach region at two wavelengths: 543.5 (the peak of the band) and 558.5 nm (the red shoulder). Figures 3a and 4a show data for pump wavelengths of 683 and 661 nm, respectively. Insets show the early time behavior. Also included in the inset to Figure 4a is a weak subpicosecond transient near $t = 0$. This is the response of the buffer/glycerol solution at low temperature with a probe wavelength of 543.5 nm and under the same excitation conditions as the RC data. Similar transients occur at 558.5 nm and with 683 nm excitation (data not shown). Transients of comparable amplitude and time scale are found in the RC data; it is therefore likely that the subpicosecond decay

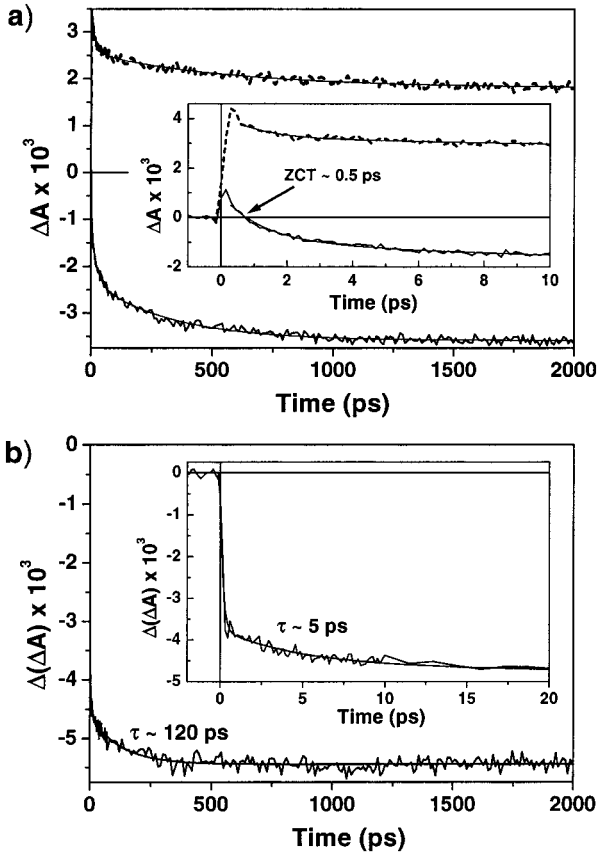

Figure 3. (a) Transient absorption kinetics at 543.5 and 558.5 nm (solid and dashed data lines, respectively) for the isolated PSII RC complex at 7 K (λ_{exc} = 683 nm, 100 nJ). Inset shows the data at early time, with the zero crossing time indicated. The triple exponential fits to the data (thin solid lines, see Table 1) are also shown. (b) 543.5 nm minus 558.5 nm (i.e., bleach growth) kinetics showing the growth of the Pheo Q_x band bleach and its fit to 5 and 120 ps components. Inset shows early time behavior.

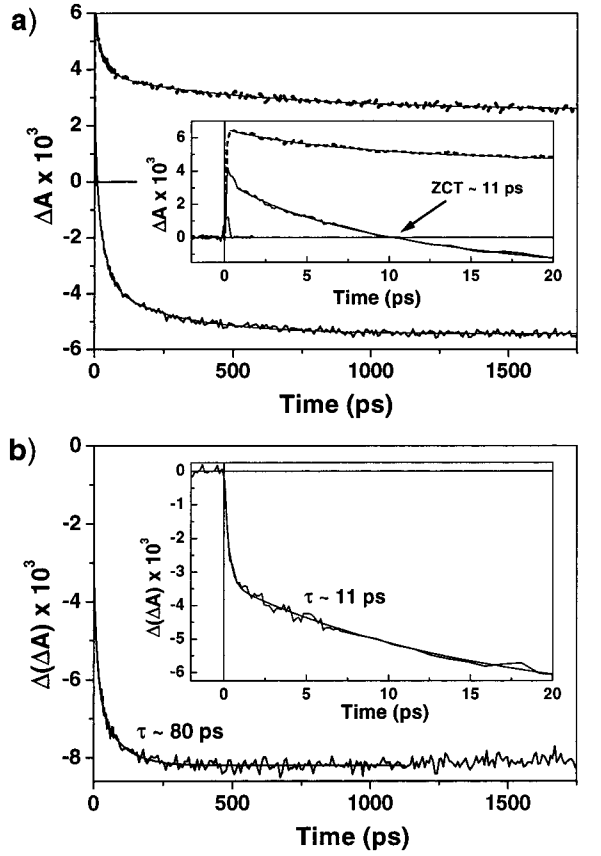

Figure 4. (a) Transient absorption kinetics at 543.5 and 558.5 nm (solid and dashed data lines, respectively) for the isolated PSII RC complex at 7 K (λ_{exc} = 661 nm, 100 nJ). Inset shows the data at early time, with the zero crossing time indicated. The weak subpicosecond transient near $t = 0$ is the response of the buffer/glycerol solution (see text). The triple exponential fits to the data (thin solid lines, see Table 1) are also shown. (b) 543.5 nm minus 558.5 nm (i.e., bleach growth) kinetics showing the growth of the Pheo Q_x band bleach and its fit to 11 and 80 ps components. Inset shows early time behavior.

in the RC data is merely the response of the solvent, and as such, is unrelated to RC kinetics. Hence, fits are started after this component has decayed, typically 300−400 fs after the peak. Similar to the case at 278 K, three decaying exponential components plus a nondecaying (on a 1 ns time scale) component are required to fit the data at either probe wavelength. Table 1 summarizes the results of fits to the raw data. For comparison, Table 1 includes the fits to the 278 K data from ref 33.

As with the case of the 278 K data, we believe that an analysis of the growth of the bleach is far more informative than trying to interpret single-wavelength data taken at the peak of the bleach. However, before examining the bleach growth, a few aspects of the raw data merit discussion. Overall, the fit parameters for the different temperatures and excitation and probe wavelengths are fairly similar. Only the time constant for the slow component changes appreciably between 543.5 and 558.5 nm; in all cases, it is faster at the peak of the Pheo Q_x bleach that at its shoulder (by a factor of approximately two at 7 K).

As a function of excitation wavelength at 7 K, the time constants of the intermediate and slow components do not change within experimental error. However, the faster component speeds up by a factor of 2 going from blue- to red-pool excitation. There is also a shift from a relatively dominant (∼50%) intermediate component with blue-pool excitation to a fairly even distribution of the amplitudes across the three components with red-pool excitation.

There is a greater degree of change to the fit parameters in going from 278 K to 7 K. Although the fast and intermediate time constants appear to be temperature independent (to within experimental error), there is a dramatic difference in the slow component. At low temperature, this component is slower by a factor of 3−4 than at 278 K. There is also a shift from a relatively dominant (∼50%) intermediate component at 278 K to a fairly even distribution of the amplitudes across the three components at 7 K. This amplitude change is virtually identical to the one seen in going from blue- to red-pool excitation at 7 K.

As was the case at 278 K,[37] the most dramatic difference in the data as a function of excitation wavelength is the "zero-crossing time" (ZCT), the time at which the transient crosses $\Delta A = 0$ when probing at the peak of the Pheo Q_x band. At 278 K, we showed that this time is a sensitive indicator of a number of parameters, including sample quality, excitation fluence (i.e., the degree of multiple excitation of individual RCs), and the pigment pool being excited.[37] At the lowest excitation energies (at which negligible multiple excitations should occur), a ZCT of ∼10 ps was found for red-pool excitation at 278 K. In contrast, at 7 K, the equivalent ZCT is ∼500 fs. For blue-pool excitation, the ZCT is ∼23 and ∼12 ps for 278 and 7 K, respectively. Thus, for both excitation wavelengths, the ZCT is ∼10 ps earlier at 7 K than at 278 K. At 278 K, the ZCT increases with either increasing excitation fluence or decreasing

TABLE 1: Averages and Estimated Errors for the Fit Parameters to the Data at the Peak of the Pheo Q_x Band (543.5 nm) and at Its Red Shoulder (558.5 nm)[a]

T (K)	λ_{pump} (nm)	λ_{probe} (nm)	A_{fast}	τ_{fast} (ps)	A_{int}	τ_{int} (ps)	A_{slow}	τ_{slow} (ps)	$A_{shelf} \times 10^3$	ZCT (ps)
7	661	543.5	$(25 \pm 4)\%$	4 ± 1	$(53 \pm 2)\%$	29 ± 4	$(22 \pm 3)\%$	280 ± 60	-4.4 ± 0.8	11.5 ± 1.5
		558.5	$(26 \pm 5)\%$	4 ± 1	$(41 \pm 3)\%$	46 ± 10	$(33 \pm 3)\%$	770 ± 230	2.2 ± 0.3	N/A
	683	543.5	$(38 \pm 2)\%$	2 ± 1	$(31 \pm 2)\%$	24 ± 8	$(31 \pm 2)\%$	310 ± 50	-4.6 ± 0.8	0.5 ± 0.2
		558.5	$(36 \pm 4)\%$	2 ± 2	$(30 \pm 3)\%$	35 ± 25	$(34 \pm 3)\%$	640 ± 250	1.9 ± 0.3	N/A
278	687	543.0	$(24 \pm 5)\%$	3 ± 1	$(51 \pm 3)\%$	20 ± 5	$(24 \pm 6)\%$	100 ± 20		10.2 ± 0.5
		558.0	$(30 \pm 9)\%$	3 ± 1	$(51 \pm 6)\%$	20 ± 5	$(20 \pm 4)\%$	140 ± 20		N/A

[a] Estimated errors are the standard deviations of individual data set fit parameters. The zero-crossing time (ZCT) is the time at which the transient crosses $\Delta A_{543.5nm} = 0$ (measured after the peak of the transient). The shelf refers to the nondecaying (on a 1 ns time scale) component of the data. Component amplitudes (other than that of the shelf) are reported as a percentage of the total amplitude. The 278 K fits are from the data of ref 33, although these fits were not presented in that paper. Shelf amplitudes are not reported for the 278 K data, as the excitation intensity was varied from 30 to 100 nJ between scans. The excitation energy was kept constant at 100 nJ for the 7 K data.

sample quality. At 7 K, the ZCT clearly increases with sample degradation (see Figure 7a, section 3.4). However, it is difficult to determine the intensity dependence of the ZCT at low temperature, as high excitation energies rapidly result in sample degradation.

3.3. Bleach Growth Analysis. In our work at 278 K,[33] we argued that the kinetics of the depletion of ground-state Pheo could not be measured with kinetic data taken solely at the peak of the Pheo Q_x bleach. This contention was based on the substantial time-dependent shift of the transient spectra to lower ΔA values over the entire 500−600 nm region (rather than just within the Pheo Q_x band); that is, the baseline was shifting. Similarly, at 7 K, this shift is of comparable magnitude and occurs on the same time scale as the changes in the Pheo Q_x band. We showed that this behavior was completely different from that of the RC complex isolated from the photosynthetic bacterium *Rb. sphaeroides* R26, for which there was very little change in the same spectral region (except of course in the Pheo Q_x band itself).[33] Whereas a single-wavelength measurement for the bacterial RC complex could accurately measure the kinetics of Pheo ground-state depletion, such is not possible for the PSII RC complex. A single-wavelength kinetic measurement of the PSII RC at 543.5 nm would include a significant contribution due to the changing background, which may be completely unrelated to the kinetics of charge separation. However, we believe that a measurement of the kinetics of the changing background can be used to correct the kinetics measured at 543.5 nm for this phenomenon.

Ideally, one would like to measure the changing background at the peak of the Pheo Q_x bleach. Since this is not possible, we need to determine which wavelength would best mimic the changing background at 543.5 nm. Arguments related to this issue are the same as presented earlier[33] and will only be summarized. The effect of any wavelength dependence in the changing background is minimized by using a probe wavelength as close to 543.5 nm as possible, so long as this wavelength is outside of the Pheo Q_x band itself. This makes the shoulders of the Pheo Q_x band the best choice for measuring the changing background. Since the blue shoulder may be affected by the vibrational sideband of the Pheo Q_x transition, the red shoulder (at 558.5 nm) was used as the wavelength to measure the changing background. Because the bleach is narrower at cryogenic temperatures, we could have used a reference wavelength that was a few nanometers closer to the peak than was done at 278 K; however, for consistency, we chose to use the same +15 nm shift as was used in ref 33. It is highly unlikely that the behavior of the background would change significantly over these 15 nm, since the absorption spectra of both chlorin excited singlet states[37,40] and ion radical states[41,42] are rather broad and featureless throughout this part of the visible spectrum. Finally, the validity of this method was supported by the agreement of the bleach growth analysis with single-wavelength data in the Pheo anion band region (where the changing background is much smaller) at 278 K.[33]

The effect of removing the changing background (as measured at 558.5 nm) can be seen in Figures 1b and 2b for pump wavelengths of 683 and 661 nm, respectively. These data were generated by translating each spectrum in Figures 1a and 2a along the *y*-axis by the necessary amount to set $\Delta A_{558.5nm} = 0$ at all times. With this manipulation accomplished, the growth of the Pheo Q_x bleach now stands out as the dominant feature that changes as a function of delay time. On the other hand, little change with time is seen in the Chl Q_x band centered at ~584 nm (with the exception of the 0.5 ps spectrum of Figure 1b, which may well be an artifact of imperfect compensation for the chirp on the probe beam). The increase of the Pheo Q_x bleach beyond its instantaneous amplitude is significantly greater for 661 nm excitation (Figure 2b) than for 683 nm excitation (Figure 1b). There is also a substantially greater degree of change in the 500−530 nm region for 661 nm excitation than for 683 nm excitation. As this wavelength region is dominated by the Pheo Q_x vibrational sideband centered at ~512 nm, this may simply be a reflection of the greater degree of noninstantaneous Pheo Q_x bleach growth that occurs with blue-pool excitation.

The bleach growth kinetic data were generated by subtracting the 558.5 nm data from the 543.5 nm data from single experimental runs on the same sample. Furthermore, the vast majority of the bleach growth data sets were created from consecutively acquired 543.5 and 558.5 nm data sets. Figures 3b and 4b show bleach growth data for pump wavelengths of 683 and 661 nm, respectively. The data are fit to an instrument response-limited component and an ensuing biexponential rise to a nondecaying shelf. A small decay (a few percent) in the shelf is discernible in the 1−2 ns region. This decay is completely consistent with the $(100\ ns)^{-1}$ rate constant for radical pair recombination measured by van Kan et al. at 10 K.[39] Since fitting data that extend out to only 2 ns with a ~100 ns decay constant makes no sense, no attempt was made to do so. Instead, the fits were truncated at the point at which the data began to decay (typically 1.2 ns). The results of our bleach growth fits are summarized in Table 2. For comparison, the 278 K bleach growth data from ref 33 is also included here.

3.4. Photodegradation. The sample is extremely stable with 100 nJ excitation pulses. However, degradation occurs rapidly with ~1 μJ or greater excitation pulses, especially when exciting into the red pigment pool. Figure 5 shows absorption spectra at 7 K of a fresh spot and of the same spot after various durations of exposure to 1.0 μJ, 683 nm excitation pulses. The absorption peak at ~679 nm progressively disappears; little change is observed in either the blue side of the composite Q_y band or the broad vibrational sideband centered at ~625 nm. The inset

TABLE 2: Averages and Estimated Errors for the Fit Parameters to the Bleach Growth Data (543.5 nm Data Minus 558.5 nm Data, See Figures 3b and 4b)[a]

T (K)	λ_{pump} (nm)	A_{IR}	τ_{fast} (ps)	A_{fast}	τ_{slow} (ps)	A_{slow}	A_{slow}/A_{fast}	$A_{shelf} \times 10^3$
7	661	(38 ± 6)%	11 ± 4	(35 ± 9)%	80 ± 40	(27 ± 8)%	0.9 ± 0.6	7.0 ± 1.0
	683	(66 ± 7)%	5 ± 1	(18 ± 4)%	120 ± 40	(16 ± 3)%	0.9 ± 0.1	6.4 ± 0.9
278	687	(41 ± 5)%	9 ± 2	(28 ± 6)%	54 ± 8	(31 ± 4)%	1.1 ± 0.3	

[a] Estimated errors are the standard deviations of individual data set fit parameters. A_{IR} is the amplitude of the instrument response-limited component. The shelf refers to the nondecaying (on a 1 ns time scale) component of the data. Component amplitudes (other than that of the shelf) are reported as a percentage of the total amplitude. The 278 K data are from ref 33; shelf amplitudes are not reported for those data, as the excitation intensity was varied from 30 to 100 nJ between scans. The excitation energy was kept constant at 100 nJ for the 7 K data.

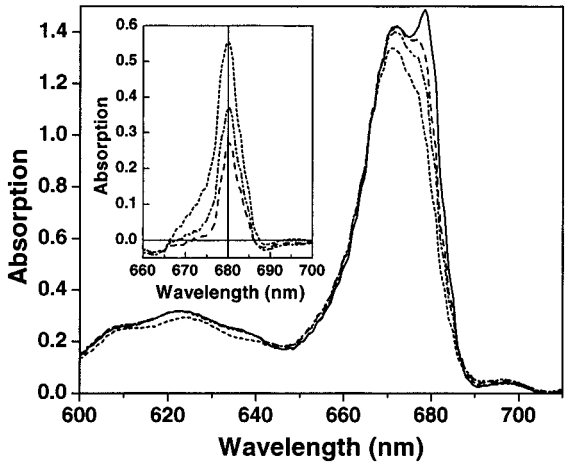

Figure 5. Steady-state absorption spectra of the composite Q_y band of the isolated PSII RC complex at 7 K. Solid line is the spectrum of a fresh spot. Other lines are the spectra of that spot after various durations of exposure to 1.0 μJ, 683 nm pulses, showing the gradual loss of the red peak. Inset shows the differences between the spectrum of the fresh spot and the spectra of the degraded samples.

to the figure shows the differences between the spectra of the fresh and degraded spots. These difference spectra, which peak at 680 nm and have a fwhm of ~5.5 nm (120 cm^{-1}), represent the species that is being destroyed, presumably P680.

It is quite possible that the degradation rate is the same near room temperature. However, the sample suspensions for our 278 K experiments[33,37] were stirred for the expressed purpose of mixing the sample and therefore dramatically reducing the number of excitations that any single RC would experience over the course of a scan. As mentioned above, at 7 K the same RCs were illuminated over the entire course of a scan since the sample was not rastered.

Transient spectral and kinetic data were also acquired on a sample degraded with 683 nm light. The sample for these experiments was degraded by 115 min of exposure to 1.35 μJ pulses at 400 Hz (roughly 2.8 million pulses). This resulted in an absorbance loss of 0.46 at 680 nm (almost as much as for the final spectrum in Figure 5). The majority of the degradation occurred relatively quickly; the absorbance loss was only 0.05 over the final 65 min, indicating that the degradation process was fairly complete at the end. As can be seen from Figure 5, the degradation has negligible effect on the sample absorbance at the 661 nm excitation wavelength used for the transient experiments performed on this sample.

Figure 6a shows transient absorption spectra of this degraded sample at several delay times. The changing background in the transient spectra is still clearly visible. Figure 6b shows the growth of the Pheo Q_x bleach, with the data manipulated as was done for Figures 1b and 2b (see section 3.3). Figure 7 compares kinetic data from this damaged sample with that of an active sample at probe wavelengths of both 543.5 and 558.5 nm. Although the active and damaged kinetics are identical for

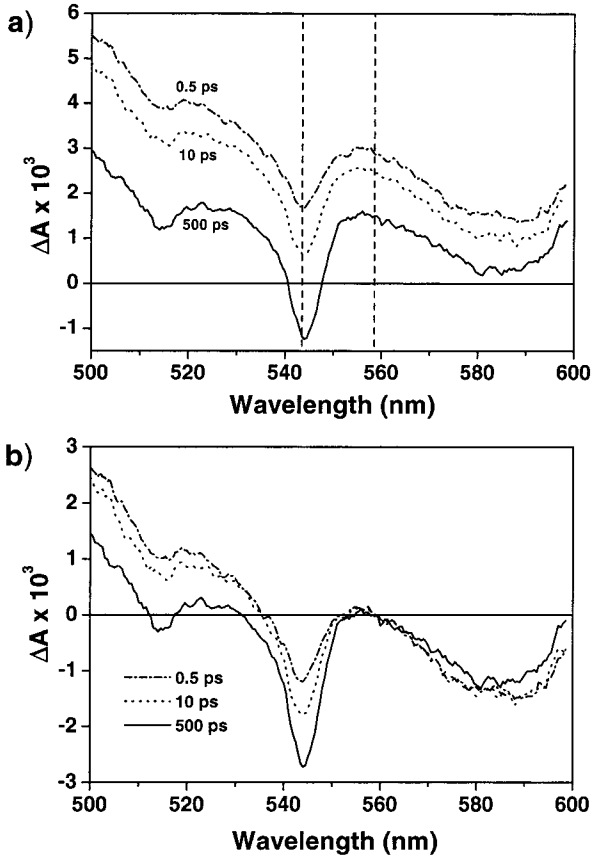

Figure 6. (a) Transient absorption spectra of the isolated PSII RC complex at 7 K recorded at 0.5, 10, and 500 ps after a 100 nJ, 661 nm excitation pulse. The sample has been damaged with exposure to 1.35 μJ pulses at a wavelength of 683 nm (see text and Figure 5). Dashed vertical lines show the 543.5 and 558.5 nm probe wavelengths used for the bleach-growth analysis. (b) Same data as in (a), but with the data vertically shifted to set $\Delta A_{558.5nm} = 0$ at all three delay times.

the first picosecond, they strongly diverge at later time. The bleach growth kinetics for the two samples are also shown in Figure 7. The bleach growth of the damaged sample can be well fit to a single-exponential rise (following the instantaneous component) with a time constant of ~26 ps. A reduction in the final bleach amplitude by a factor of approximately 2 due to the degradation is clearly apparent.

4. Discussion

4.1. 683 nm Excitation. A significant majority (two-thirds) of the final amplitude of the Pheo Q_x bleach occurs during the excitation pulse. This represents a significant increase over that seen at 278 K (41%).[33] The large initial bleach at 7 K is a significant result, providing important insight into the nature of the electronic structure of P680. Explanations for this large initial bleach that are consistent with a dimer model of P680 do not seem credible, as will be discussed below. However, the large

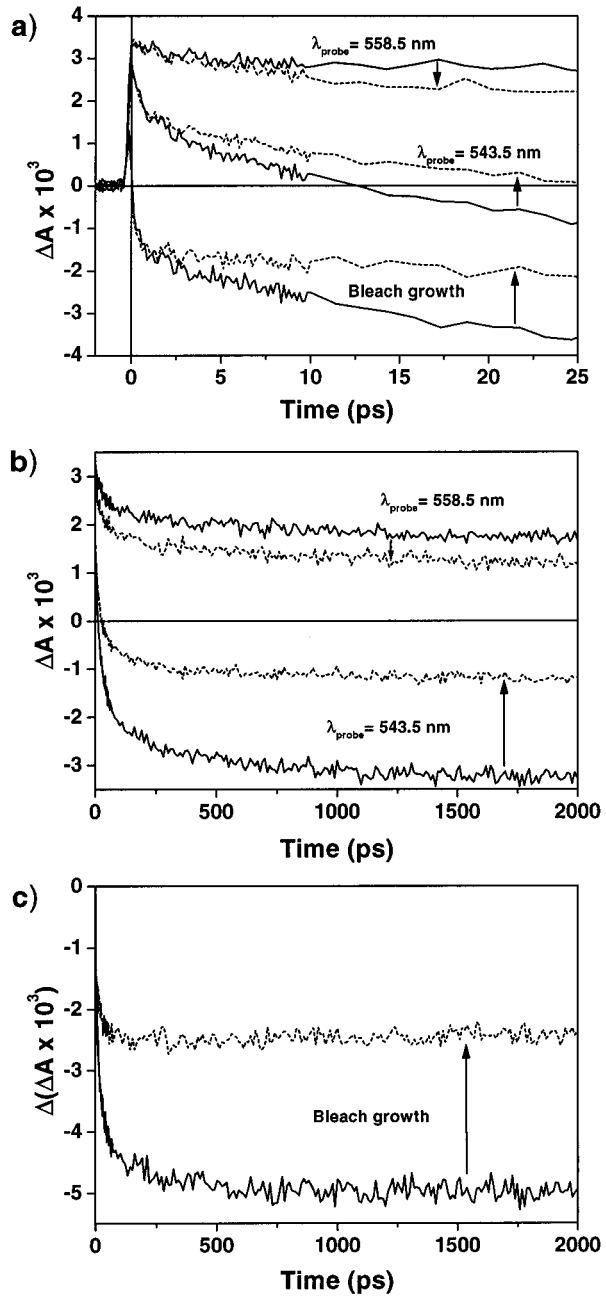

Figure 7. Transient absorption kinetics at 543.5 and 558.5 nm for the isolated PSII RC complex at 7 K (λ_{exc} = 661 nm, 100 nJ). Solid lines are of an active sample; dashed lines are of a sample that has been damaged with exposure to 1.35 μJ pulses at a wavelength of 683 nm (see text and Figure 5). Also shown are the bleach growth kinetics generated from these data sets. Arrows indicate the direction of the changes in the data from active to degraded samples. (a) Early time behavior. The data are indistinguishable for the first picosecond, but rapidly diverge thereafter. Note the increase in the zero-crossing time for the 543.5 nm data. (b) Long time behavior of the single-wavelength kinetics. (c) Long time behavior of the bleach growth kinetics.

initial bleach is anticipated by a multimer model that includes the Pheos as components of the multimer,[9−13] since any absorption by the multimer would result in significant instrument response-limited Pheo ground-state depletion. (Recall that the Pheo Q_x bleach is a measure of ground-state depletion, and can be caused by the generation of either ^{1*}Pheo or Pheo$^-$). This result therefore strongly supports a multimer model of P680.

Within the context of the dimer model for P680, explanations for the large initial Pheo Q_x bleach do not appear plausible. It is not possible to form a large population of ^{1*}Pheo from direct absorption by Pheo, as the fraction of the red-pool oscillator strength that belongs to Pheo is relatively small (17%, if the red pool consists of the active Pheo and three Chls, given a Pheo/Chl extinction coefficient ratio of 0.6:1). Comparison of the kinetics of active and degraded samples (see section 4.3) appears to rule out ultrafast (a few hundred femtoseconds or less) charge separation as a possible explanation. Finally, the formation of a ^{1*}Pheo "bottleneck" state by ultrafast energy transfer also seems unlikely, as it would involve substantial ground-state depletion of P680 (i.e., bleaching of the Chl bands) occurring on the time scale of charge separation (i.e., a few picoseconds or longer). This is inconsistent with both our results in the Chl Q_x band (see Figure 1b) and the results of others in the Q_y band at 20 K (as well as at higher temperatures).[36]

Calculations by Durrant et al.[10] showed that localization of the multimer excited state on an individual pigment (i.e., anion, cation, or triplet formation) results in a loss of oscillator strength (relative to the ground-state) in the composite Q_y band. Furthermore, the amount of oscillator strength lost depends on the identity of the pigment upon which the excitation is localized, even differing for different Chls.[10] Without detailed calculations, it is not obvious to what extent localization due to Pheo anion formation would result in additional loss of Pheo Q_x oscillator strength beyond that bleached by the multimer exciton. Nevertheless, this seems the most likely explanation for the 5 ps component of the bleach growth, which we therefore assign as the intrinsic time constant for charge separation. This is entirely consistent with the (8 ps)$^{-1}$ rate constant measured at 278 K.[33] The uphill energy transfer that causes the equilibration of the RC core at 278 K should be essentially shut off at 7 K. This would result in the localization of the excitation energy on the lowest energy multimer state and would appear as an increase in the measured rate constant for charge separation.

There also exists a much slower (120 ps) component to the bleach growth at 7 K that contributes ∼16% to the final Pheo Q_x bleach amplitude. There are certainly numerous plausible explanations for this; the data are unable to unambiguously distinguish which is correct. Several will be discussed below, concentrating on previously proposed models that account for the multiexponential kinetics at higher temperatures.

At 278 K, with preferential excitation of P680 at 687 nm, we also observed biphasic bleach growth kinetics. The slower component (50 ps) was assigned to charge separation limited by slow energy transfer from a long-wavelength monomeric Chl.[33] A similar explanation was given by Groot et al.[36] for their 120 ps component at 20 K with 685 nm excitation. The presence of a trap ∼1 nm to the red of P680 with a lifetime of 4 ns for a ∼6-Chl preparation was confirmed by hole burning experiments.[43] However, the thermal energy (k_BT) at 7 K is only 5 cm^{-1} (0.6 meV). For a 1 nm (22 cm^{-1}) energy gap, the Boltzmann term decreases the rate constant of an activated process at 7 K relative to 20 K and 278 K by a factor of 18 and 76, respectively. Therefore, a detrapping mechanism appears questionable for the slow component at 7 K. However, this does not preclude detrapping from being the correct explanation for the slow component at elevated temperatures.

Relaxation of the charge-separated state has been suggested as the source of the nonexponential kinetics observed in the PSII RC near room temperature[13,26,27] and at 77 K.[44] This may be structural relaxation of the protein matrix (similar to the dynamic solvation that has been suggested by Woodbury and co-workers for bacterial RCs[45]) or subsequent charge separation reactions following the formation of the initial charge-separated

state. In either case, back electron transfer sets up an equilibrium between ^{1*}P680 and the (first) charge-separated state, with the relaxation process gradually shifting the equilibrium away from ^{1*}P680. For this model to be operative, the thermal energy must be at least comparable to the instantaneous free energy gap between the aforementioned states. However, the thermal energy at 7 K is extremely low (vide supra), requiring that these states be virtually degenerate.

Although Klug and co-workers[13] have presented calculations that indicate that dispersive kinetics in PSII RCs cannot be explained by heterogeneity in either the energy gap or coupling constants, there still exists a very active debate on this same issue for the much easier to study bacterial RC.[46−49] It therefore seems premature to rule out heterogeneity as the explanation for the existence of the slow component.

Another possible explanation for the slow component is energy transfer to trap Pheo. The trap shows signs of containing contributions from Pheo as well as Chl.[43] If energy transfer were to occur to a trap Pheo, it would appear as an increase in the depth of the Pheo Q_x bleach, which would be consistent with our observation. Thus, the slow component may be completely unrelated to any processes that result in charge separation at low temperature.

As discussed above, localization of the multimer excited state on Pheo may result in additional loss of Pheo Q_x oscillator strength. The magnitude of this effect can be estimated as follows. If we assume negligible direct absorption from a long-wavelength Chl and/or negligible detrapping from that pigment, then $Pheo^-$ (and any $^{1*}Pheo_{trap}$) is formed only from directly excited multimer excitons. Therefore, ∼66% (i.e., the fraction of the bleach occurring instantaneously) of the Pheo Q_x oscillator strength is bleached by formation of the multimer excited state, with the remainder bleached by localization on Pheo. However, if we assume that the slow component to the bleach growth is due to charge separation following detrapping from a long-wavelength Chl (vide supra), then only the 5 ps component of the bleach growth is due to localization from directly excited multimer excitons. In this case, the effect of localization should be estimated by the ratio of the initial bleach to that bleached *before* the slow component; i.e., $0.66/(0.66 + 0.18) = 79\%$.

4.2. 661 nm Excitation: Active Samples. The amplitude of the initial Pheo Q_x bleach with 661 nm excitation is a substantially smaller percentage of the final bleach depth than with 683 nm excitation, (38 ± 6)% vs (66 ± 7)%. This is entirely consistent with the multimer model for the PSII RC. Blue-pool excitation will result in the direct excitation of two distinct populations: the blue core pigments (i.e., the higher energy exciton states of the multimer[10]) and the peripheral Chl-(s). Slow energy transfer is known to occur upon selective excitation of the blue pigment pool,[24,25,37,50] presumably from the peripheral Chl(s) to the RC core. The proponents of the multimer model argue that both (as opposed to only one) of the peripheral Chls absorb near 670 nm.[19] Therefore, a sizable fraction of the absorption with blue-pool excitation would be from the peripheral Chls, and these RCs will contribute to the Q_x bleach only after the slow energy transfer to the multimer core. On the other hand, those RCs that experience direct excitation of the core will have partial instantaneous bleaching of their Pheo Q_x band. Let us assume that for 683 nm excitation, all of the absorption is due to the multimer and the observed initial bleach of 66% is entirely due to the multimer exciton. This would indicate that ∼58% (0.38/0.66) of the absorption at 661 nm is due to the multimer core, with the remainder due to the peripheral Chls.

Preferential excitation of the pigments on the blue side of the composite Q_y band at 661 nm indeed results in biphasic bleach growth kinetics. The faster component with 661 nm excitation is 11 ± 4 ps, a factor of more than 2 slower than with preferential direct excitation of P680. However, given the 683 nm data and the model for blue-pool excitation discussed above, a 5 ps phase should exist: directly excited blue core pigments should lead to charge separation with virtually the same time constant that is observed with red-pool excitation. Thus, the 11 ps phase may be a composite with a contribution from charge separation following ultrafast energy transfer and a contribution from charge separation following slow energy transfer. To test this, we have tried refitting the 661 nm excitation bleach growth data by adding a 5 ps phase to the fit. The rise of the bleach growth is therefore fit to three exponential components plus the instrument response-limited rise, with the extra component having a fixed 5 ps time constant but a variable amplitude. Under these conditions, the three time constants are 5 ps, ∼22 ps, and ∼130 ps. This puts the time constant for the slowest component very close to the 120 ps value measured with 683 nm excitation. Furthermore, the amplitude percentage of slowest component is significantly reduced, becoming nearly identical for the two excitation wavelengths (∼15%). The kinetics with blue-pool excitation are therefore described as follows. The 5 ps component corresponds to charge separation following subpicosecond energy transfer to the lowest energy multimer state. The 22 ps component corresponds to charge separation limited by slow energy transfer from the peripheral Chl(s). Finally, the 130 ps component corresponds to the same process that causes that component with red-pool excitation (see section 4.1).

Transient absorption spectra at 2 ns represent the "stable" charge-separated state $P680^+-Pheo^-$, with some contribution from excited trap states (see section 4.1). The spectra with 661 and 683 nm excitation wavelengths are qualitatively identical at this time, indicating that the RCs are in the same state(s) independent of excitation wavelength. Since these excitation wavelengths were chosen to give roughly the same sample absorbance, this implies that the quantum yield for energy transfer from the blue to the red pigment pools is near unity at 7 K, as we had previously seen near room temperature.[37] This is quantitatively supported by the kinetic data. The signal levels at long time (as measured by the shelf amplitudes) at both probe wavelengths are identical for blue- and red-pool excitation to within experimental error. It should be noted, however, that no estimate of the quantum yield for charge separation is made.

Figure 8 shows spectral data of the Pheo Q_x bleach at 1.0 ps and 2.0 ns with 661 nm excitation. These data have been normalized at the peak of the bleach after the bleach growth correction (see Figure 2b). Both the width of the bleach (∼7.0 nm fwhm) and the position of the peak are invariant with time. The peaks of the Q_x bands for the inactive and active Pheos at low temperature are at 541.2 and 544.4 nm, respectively.[16] Since the Q_y bands for the inactive and active Pheos are at roughly 670[6,15,16] and 681 nm,[14−16] respectively, 661 nm excitation should result in the direct excitation of only the inactive Pheo and Chls. At long time (i.e., 2 ns), however, the bleach is presumably due solely to the active Pheo. Since the Pheo Q_x bleach in the 2 ns spectrum shows no evidence of either narrowing or blue-shifting with respect to the bleach in the 1 ps spectrum, it appears that there is negligible population of $^{1*}Pheo_{inactive}$ at the earlier time. This is a clear indication that the inactive Pheo undergoes ultrafast energy transfer to the red side of the band (including to the active Pheo).

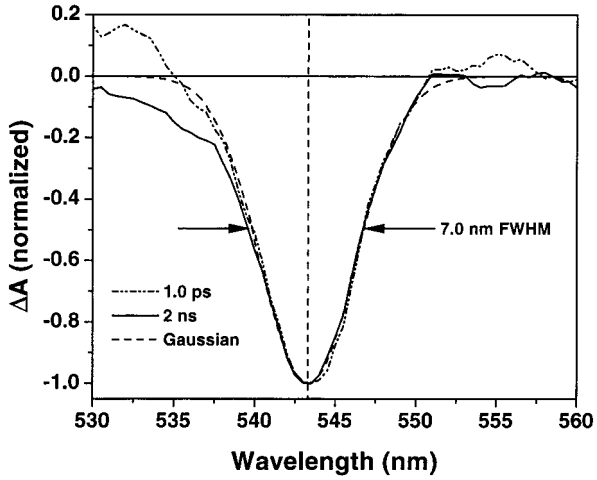

Figure 8. Transient absorption spectra of the Pheo Q_x band at 1.0 ps and 2.0 ns after a 100 nJ, 661 nm excitation pulse. The data have been normalized at the peak of the bleach after the manipulation that compensates for the changing background (see text and Figure 2b). Also shown for comparison is a 100 cm^{-1} Gaussian. Arrows indicate the ~7.0 nm fwhm.

4.3. Degraded Samples. One would expect that the primary effect of the photodegradation would be damage to P680, resulting in the disruption of charge separation. Since the active Pheo would presumably remain undamaged, ^{1*}Pheo could continue to be formed and might become a major trap for the excitation energy. This is consistent with the continued presence of a Pheo Q_x bleach with these samples; see Figure 6. However, if ^{1*}Pheo were the only trap (i.e., formed in virtually all of the excited RCs), then the depth of the Pheo bleach in a damaged sample would be the same as in an active sample. (Recall that degradation with 683 nm pulses does not affect the sample absorbance at 661 nm; see Figure 5). Since the final depth of the bleach is substantially smaller than with active samples, ^{1*}Chl must also contribute to the trap.

As can be seen in Figure 7a, the kinetics for active and damaged samples are identical (to within the noise) for the first picosecond, diverging thereafter. This observation largely rules out the possibility of charge separation occurring on a subpicosecond time scale, as the kinetics would certainly diverge sooner if ultrafast charge separation were to occur in the active sample.

Experiments on samples degraded with 683 nm pulses can be used to test the validity of the "splitting" of the 11 ps component of the bleach growth into 5 and 22 ps components for active samples with 661 nm excitation (see section 4.2). With 661 nm excitation, the bleach growth of a damaged sample can be well fit to a single-exponential rise (following the instantaneous component) with a time constant of ~26 ps. This is close to the 22 ps time constant identified above for charge separation limited by slow energy transfer from the peripheral Chls in active samples. It is reasonable to expect that this energy transfer process would remain after degradation, although possibly with a modified rate constant. The disappearance of the slow component (the ~80 or ~130 ps component, depending on whether it is a two- or three-exponential fit) for the damaged sample may well indicate that this component is associated with charge separation. However, we cannot exclude the possibility that it is related to Chl-to-Pheo energy transfer that is disrupted by the degradation.

The absence in damaged samples of the 5 ps component assigned to charge separation in active samples is expected. To test whether this component was "missed" in the fit of the damaged sample data, we have refitted these data with the inclusion of an additional fixed 5 ps component (akin to what was done with active samples, see section 4.2). Unlike the case of the active samples, however, the 5 ps component of the damaged sample has negligible amplitude, and consequently the χ^2 value for the fit is not improved by the addition of this component. These results thus support the assignment of $(5\ ps)^{-1}$ as the intrinsic rate constant for charge separation.

4.4. The Nature of the Changing Background. We believe that the bleach growth analysis is the correct approach to measuring the rate constant for charge separation based on the Pheo Q_x band, as it eliminates the large changing background that would be included in a single-wavelength kinetics analysis. It is still unclear, however, what the cause of the changing background is. One possible explanation is that it is due to relaxation of the charge-separated state, be it through multiple charge-separated states or relaxation of the protein matrix around a single state (though not necessarily involving a shifting equilibrium with the excited singlet state as was discussed in section 4.1). To test whether relaxation of the charge-separated state is responsible for the changing background, we compared the transient kinetics of active and degraded samples probing at 558.5 nm (see Figure 7). As discussed above, the sample absorbance at the 661 nm excitation wavelength was not changed by exposure to the 683 nm degradation pulses. Consequently, the initial amplitude of the transient (i.e., near $t = 0$) was nearly identical for the two samples. However, the final amplitude of the degraded sample was *smaller* than that of the active one. This means that the background (as represented by the 558.5 nm kinetics) underwent a *greater* change for the degraded sample than for the active one. It therefore seems unlikely that relaxation of the charge-separated state is the source of the changing background.

4.5. Comparisons with Other Work. The faster component for the bleach growth at 7 K with 683 nm excitation is 5 ± 1 ps and presumably corresponds to direct charge separation from ^{1*}P680. This is significantly slower than other measurements made at 20 K or below: hole burning, 1.9 ps at 4.2 K, ref 18; transient absorption, 1.4 ps at 15 K, ref 34 and 2.6 ps at 20 K, ref 36. One possible explanation for the discrepancy with the sub-20 K results is that somewhat different samples were used in those early experiments. Both used samples that were isolated using significantly harsher methods than are currently employed. Furthermore, the transient absorption experiment of Wasielewski et al.[34] used excitation energies that were about 20 times greater than were used in this study. Although partially mitigated by the lower sample absorbance at their nonselective 610 nm excitation wavelength, such a high excitation energy could have caused some multiple excitations of individual RCs (possibly leading to annihilation in those RCs), and might have been high enough to result in some sample degradation. Recently, Jankowiak and co-workers[51] performed hole burning experiments on the same stock of RC material as was used in this work. There appear to be multiple contributions to the transient holes, including a component with a width that corresponds to a $(5\ ps)^{-1}$ rate constant. However, the interpretation of these results, including which component(s) corresponds to charge separation, is still in progress.

The 2.6 ps time constant for charge separation measured by Groot et al.[36] at 20 K is based on transient absorption data in the composite Q_y band. Both we[33] and others[31] have previously argued that the small Stokes shift of the stimulated emission combined with the aforementioned spectral congestion of the

Q_y band make other spectral regions better suited for determining the rate constant for charge separation.

5. Conclusion

The instantaneous bleaching of the Pheo Q_x band equal to two-thirds of the final bleach amplitude with 683 nm excitation provides compelling support for a multimer description of the PSII RC core. Studies near room temperature have also shown a substantial initial bleach, and this has been previously argued as evidence for the multimer model.[10] However, as a percentage of the final depth, the initial bleach is dramatically greater at 7 K than near room temperature. Whereas it may be possible to discount the importance of the initial bleach near room temperature, this large initial bleach at 7 K is a feature that must be successfully described by any model of the PSII RC. The large initial bleach clearly indicates that the active Pheo is a component of the multimer; however, it does not necessarily provide evidence for the specific details of the multimer model as developed by Durrant and co-workers.[10−13]

Excitation at 661 nm results in an initial Pheo Q_x bleach that is significantly smaller than that observed with red-pool excitation. This is readily explained by the absorption at 661 nm being a combination of RC core and peripheral Chl absorption; we estimate the peripheral Chl contribution to the oscillator strength to be ∼42% at that wavelength. The absence of any time-dependent narrowing and/or blue-shifting of the bleach with 661 nm excitation supports the contention that the multimer branch containing the inactive Pheo is linked to the branch with the active Pheo by subpicosecond energy transfer. Comparison of the kinetics of degraded and active samples using 661 nm excitation indicates that the rate constant for energy transfer from the blue peripheral Chl(s) to the RC core is roughly $(22\ \text{ps})^{-1}$.

The intrinsic rate constant for charge separation from the RC core appears to be $(5\ \text{ps})^{-1}$; this assignment is supported by the absence of this component in damaged samples. The nature of the slow component to the bleach growth was not resolved. Two of the possible explanations involve thermally activated processes: detrapping from a long-wavelength trap state or reformation of ^{1*}P680 from a slowly relaxing charge-separated state. While the likelihood of these processes seems somewhat questionable at 7 K, they cannot be ruled out. However, experiments can be performed at substantially lower temperatures in order to resolve this question. The full interpretation of the new hole burning experiments, combined with this work and other transient absorption studies, should clarify some of the unsettled issues related to the details of energy transfer and charge separation in the PSII RC.

Acknowledgment. This work was supported by the Divisions of Energy Biosciences and Chemical Sciences, Office of Basic Energy Sciences, U.S. Department of Energy under contracts DE-AC36-83CH10093 (M.S.) and W-31-109-Eng-38 (M.R.W.). The authors thank Dr. Ryszard Jankowiak and Prof. Gerald Small for numerous discussions about their recent unpublished results, and both them and Prof. Govindjee for stimulating discussions regarding the ideas presented in this manuscript.

References and Notes

(1) Nanba, O.; Satoh, K. *Proc. Natl. Acad. Sci. U.S.A.* **1987**, *84*, 109.
(2) Seibert, M. In *The Photosynthetic Reaction Center*; Deisenhofer, J., Norris, J. R., Eds.; Academic Press: San Diego, 1993; Vol. 1, p 319.
(3) Greenfield, S. R.; Wasielewski, M. R. *Photosynth. Res.* **1996**, *48*, 83.
(4) Durrant, J. R.; Hastings, G.; Joseph, D. M.; Barber, J.; Porter, G.; Klug, D. R. *Proc. Natl. Acad. Sci. U.S.A.* **1992**, *89*, 11632.
(5) Xiong, J.; Subramaniam, S.; Govindjee. *Photosynth. Res.* **1998**, *56*, 229.
(6) Braun, P.; Greenberg, B. M.; Scherz, A. *Biochemistry* **1990**, *29*, 10376.
(7) Chang, H.-C.; Jankowiak, R.; Reddy, N. R. S.; Yocum, C. F.; Picorel, R.; Seibert, M.; Small, G. J. *J. Phys. Chem.* **1994**, *98*, 7725.
(8) Kwa, S. L. S.; Eijckelhoff, C.; van Grondelle, R.; Dekker, J. P. *J. Phys. Chem.* **1994**, *98*, 7702.
(9) Tetenkin, V. L.; Gulyaev, B. A.; Seibert, M.; Rubin, A. B. *FEBS Lett.* **1989**, *250*, 459.
(10) Durrant, J. R.; Klug, D. R.; Kwa, S. L. S.; van Grondelle, R.; Porter, G.; Dekker, J. P. *Proc. Natl. Acad. Sci. U.S.A.* **1995**, *92*, 4798.
(11) Merry, S. A. P.; Kumazaki, S.; Tachibana, Y.; Joseph, D. M.; Porter, G.; Yoshihara, K.; Barber, J.; Durrant, J. R.; Klug, D. R. *J. Phys. Chem.* **1996**, *100*, 10469.
(12) Leegwater, J. A.; Durrant, J. R.; Klug, D. R. *J. Phys. Chem. B* **1997**, *101*, 7205.
(13) Klug, D. R.; Durrant, J. R.; Barber, J. *Philos. Trans. R. Soc. London A* **1998**, *356*, 449.
(14) Tang, D.; Jankowiak, R.; Seibert, M.; Yocum, C. F.; Small, G. J. *J. Phys. Chem.* **1990**, *94*, 6519.
(15) Mimuro, M.; Tomo, T.; Nishimura, Y.; Yamazaki, I.; Satoh, K. *Biochim. Biophys. Acta* **1995**, *1232*, 81.
(16) Jankowiak, R.; Rätsep, M.; Picorel, R.; Seibert, M.; Small, G. J. *J. Phys. Chem. B*, submitted.
(17) Döring, G.; Stiehl, H. H.; Witt, H. T. *Z. Naturforsch. B.* **1967**, *22B*, 639.
(18) Jankowiak, R.; Tang, D.; Small, G. J.; Seibert, M. *J. Phys. Chem.* **1989**, *93*, 1649.
(19) Vacha, F.; Joseph, D. M.; Durrant, J. R.; Telfer, A.; Klug, D. R.; Porter, G.; Barber, J. *Proc. Natl. Acad. Sci. U.S.A.* **1995**, *92*, 2929.
(20) Groot, M.-L.; Peterman, E. J. G.; van Kan, P. J. M.; van Stokkum, I. H. M.; Dekker, J. P.; van Grondelle, R. *Biophys. J.* **1994**, *67*, 318.
(21) Wasielewski, M. R.; Johnson, D. G.; Seibert, M.; Govindjee. *Proc. Natl. Acad. Sci. U.S.A.* **1989**, *86*, 524.
(22) Wiederrecht, G. P.; Seibert, M.; Govindjee; Wasielewski, M. R. *Proc. Natl. Acad. Sci. U.S.A.* **1994**, *91*, 8999.
(23) Roelofs, T. A.; Gilbert, M.; Shuvalov, V. A.; Holzwarth, A. R. *Biochim. Biophys. Acta* **1991**, *1060*, 237.
(24) Holzwarth, A. R.; Müller, M. G.; Gatzen, G.; Hucke, M.; Grievenow, K. *J. Lumin.* **1994**, *60/61*, 497.
(25) Schelvis, J. P. M.; van Noort, P. I.; Aartsma, T. J.; van Gorkom, H. J. *Biochim. Biophys. Acta* **1994**, *1184*, 242.
(26) Gatzen, G.; Müller, M. G.; Griebenow, K.; Holzwarth, A. R. *J. Phys. Chem.* **1996**, *100*, 7269.
(27) Müller, M. G.; Hucke, M.; Reus, M.; Holzwarth, A. R. *J. Phys. Chem.* **1996**, *100*, 9527.
(28) Hastings, G.; Durrant, J. R.; Barber, J.; Porter, G.; Klug, D. R. *Biochemistry* **1992**, *31*, 7638.
(29) Durrant, J. R.; Hastings, G.; Joseph, D. M.; Barber, J.; Porter, G.; Klug, D. R. *Biochemistry* **1993**, *32*, 8259.
(30) Donovan, B.; Walker, L. A. II; Yocum, C. F.; Sension, R. J. *J. Phys. Chem.* **1996**, *100*, 1945.
(31) Klug, D. R.; Rech, T.; Joseph, D. M.; Barber, J.; Durrant, J. R.; Porter, G. *Chem. Phys.* **1995**, *194*, 433.
(32) Donovan, B.; Walker, L. A. II; Kaplan, D.; Bouvier, M.; Yocum, C. F.; Sension, R. J. *J. Phys. Chem. B* **1997**, *101*, 5232.
(33) Greenfield, S. R.; Seibert, M.; Govindjee; Wasielewski, M. R. *J. Phys. Chem. B* **1997**, *101*, 2251.
(34) Wasielewski, M. R.; Johnson, D. G.; Govindjee; Preston, C.; Seibert, M. *Photosynth. Res.* **1989**, *22*, 89.
(35) Visser, H. M.; Groot, M.-L.; van Mourik, F.; van Stokkum, I. H. M.; Dekker, J. P.; van Grondelle, R. *J. Phys. Chem.* **1995**, *99*, 15304.
(36) Groot, M. L.; van Mourik, F.; Eijckelhoff, C.; van Stokkum, I. H. M.; Dekker, J. P.; van Grondelle, R. *Proc. Natl. Acad. Sci. U.S.A.* **1997**, *94*, 4389.
(37) Greenfield, S. R.; Seibert, M.; Govindjee; Wasielewski, M. R. *Chem. Phys.* **1996**, 279.
(38) Greenfield, S. R.; Wasielewski, M. R. *Opt. Lett.* **1995**, *20*, 1394.
(39) van Kan, P. J. M.; Otte, S. C. M.; Kleinherenbrink, F. A. M.; Nieveen, M. C.; Aartsma, T. J.; van Gorkom, H. J. *Biochim. Biophys. Acta* **1990**, *1020*, 146.
(40) Shepanksi, J. F.; Anderson, R. W., Jr. *Chem. Phys. Lett.* **1981**, *78*, 165.
(41) Fujita, I.; Davis, M. S.; Fajer, J. *J. Am. Chem. Soc.* **1978**, *100*, 6280.
(42) Davis, M. S.; Forman, A.; Fajer, J. *Proc. Natl. Acad. Sci. U.S.A.* **1979**, *76*, 4170.
(43) Groot, M. L.; Dekker, J. P.; van Grondelle, R.; den Hartog, F. T. H.; Völker, S. *J. Phys. Chem.* **1996**, *100*, 11488.

(44) Konermann, L.; Gatzen, G.; Holzwarth, A. R. *J. Phys. Chem. B* **1997**, *101*, 2933.

(45) Peloquin, J. M.; Williams, J. C.; Lin, X.; Alden, R. G.; Taguchi, A. K. W.; Allen, J. P.; Woodbury, N. W. *Biochemistry* **1994**, *33*, 8089.

(46) Woodbury, N. W.; Peloquin, J. M.; Alden, R. G.; Lin, X.; Lin, S.; Taguchi, A. K. W.; Williams, J. C.; Allen, J. P. *Biochemistry* **1994**, *33*, 8101.

(47) Holzwarth, A. R.; Müller, M. G. *Biochemistry* **1996**, *35*, 11820.

(48) Laible, P. D.; Greenfield, S. R.; Wasielewski, M. R.; Hanson, D. K.; Pearlstein, R. M. *Biochemistry* **1997**, *36*, 8677.

(49) Hartwich, G.; Lossau, H.; Michel-Beyerle, M. E.; Ogrodnik, A. *J. Phys. Chem. B* **1998**, *102*, 3815.

(50) Rech, T.; Durrant, J. R.; Joseph, D. M.; Barber, J.; Porter, G.; Klug, D. R. *Biochemistry* **1994**, *33*, 14768.

(51) Jankowiak, R. Private communication.